

Detecting Contaminants in Water Based on Full Scattering Profiles within the Single Scattering Regime

Alon Tzroya, Shoshana Erlich, Hamootal Duadi, and Dror Fixler*

Cite This: *ACS Omega* 2023, 8, 23733–23738

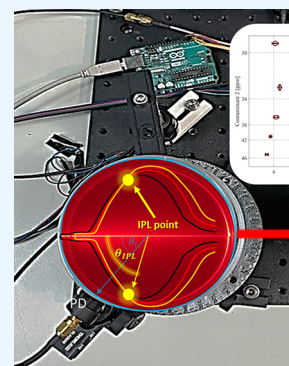
Read Online

ACCESS |

Metrics & More

Article Recommendations

ABSTRACT: Clean water is essential for maintaining human health. To ensure clean water, it is important to use sensitive detection methods that can identify contaminants in real time. Most techniques do not rely on optical properties and require calibrating the system for each level of contamination. Therefore, we suggest a new technique to measure water contamination using the full scattering profile, which is the angular intensity distribution. From this, we extracted the iso-pathlength (IPL) point which minimizes the effects of scattering. The IPL point is an angle where the intensity values remain constant for different scattering coefficients while the absorption coefficient is set. The absorption coefficient does not affect the IPL point but only attenuates its intensity. In this paper, we show the appearance of the IPL in single scattering regimes for small concentrations of Intralipid. We extracted a unique point for each sample diameter wherein light intensity remained constant. The results describe a linear dependency between the angular position of the IPL point and the sample diameter. In addition, we show that the IPL point separates the absorption from the scattering, which allows the absorption coefficient to be extracted. Eventually, we present how we used the IPL point to detect the contamination levels of Intralipid and India ink in concentrations of 30–46 and 0–4 ppm, respectively. These findings suggest that the IPL point is an intrinsic parameter of a system that can be used as an absolute calibration point. This method provides a new and efficient way of measuring and differentiating between various types of contaminants in water.



1. INTRODUCTION

Access to safe, clean water is essential for drinking, hygiene, and public health.¹ Currently, real-time water quality is primarily monitored using turbidity measurements, which assess the presence of contaminants and determine the safety of the water based on the concentration of these substances.¹ Turbidity indicates the extent to which the light is scattered or absorbed by suspended particles in the water.² Higher turbidity readings indicate more scattering and absorption events in a sample, which correspond to a higher concentration of contaminants.³ To accurately monitor water quality, it is typically necessary to use either a nephelometer or a turbidimeter.² Nephelometers use light scattering to measure water quality, while turbidimeters use light absorption.⁴ Both devices are widely used and present similar limitations.^{3,5–7} First, these methods measure relative light intensity to extract turbidity readings, and thus cannot distinguish between contaminants.^{2,3} Second, nephelometers and turbidimeters perform poorly when measuring very small particles that scatter less light, especially when present in low concentrations.^{5,8} Finally, different nephelometers and turbidimeters may have different optical systems that can affect the accuracy of the measurements, and the use of formazin as a normalization standard can be problematic because it can become less stable as the concentration of contaminants decreases.^{3,9,10} To overcome these challenges, we suggest a

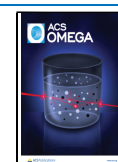
new method that relies on the optical properties of the contaminants to verify their concentration. Since the contaminants scatter and absorb light, we suggest using the full scattering profile (FSP) and utilizing the appearance of the iso-pathlength (IPL) point to accurately measure contaminant concentration. The FSP is the angular intensity distribution of light from a cylindrical medium. By incorporating numerous measurement angles, this method enhances the sensitivity for detecting scattering and absorption at low concentrations. In other words, the FSP is the intensity, I , as a function of the angle, θ , as seen in Figure 1.

The IPL point, extracted from the measurements of the FSPs, is a unique point on the surface of the sample where light intensity remains constant for a range of scattering coefficients.^{11,12} To determine the presence of the point, several measurements of the samples using the FSP are needed, with the scattering coefficient being the only variable changing between each sample.¹³ When the absorption coefficient is

Received: March 24, 2023

Accepted: June 6, 2023

Published: June 21, 2023



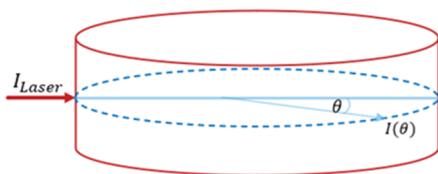


Figure 1. Light intensity (I) as a function of angle (θ).

changed but the scattering is unchanged, the IPL point will not appear.¹⁴ This implies that the IPL point allows for the separation of scattering and absorption; changes in absorption do not affect the position of the IPL point, only attenuating its intensity.^{14,15} Therefore, in order to accurately determine the position of the IPL point, the absorption coefficient must be kept constant, requiring careful sample preparation.¹⁵ It is also important to know the sample diameter because the position of the IPL point is proportional to the optical depth, which is accounted for both by the sample diameter and the distance between the detector and the sample.^{11,16} In a previous study, it was possible to isolate the absorption coefficient from the light intensity even when the scattering was unknown.¹⁵ This was due to the correction for the Beer–Lambert law with the IPL separation of the scattering from the absorption. According to the modified Beer–Lambert law:

$$\mu_a = -\frac{1}{I_{\text{IPL}} \cdot \text{DPF}} \cdot \ln\left(\frac{I(\theta_{\text{IPL}})}{I_0(\theta_{\text{IPL}})}\right) \quad (1)$$

where I_{IPL} is the geometric distance to the IPL point, $I(\theta_{\text{IPL}})$ is the intensity reading for the absorption samples, and $I_0(\theta_{\text{IPL}})$ is the intensity reading for the scattering contaminants. The DPF is the differential pathlength factor, dependent upon μ_a , μ_s , and the scattering phase function.¹⁷ Previous research on the IPL point has only been conducted on samples where light experiences multiple scattering events, known as the multiple scattering regime (the measured point is larger than $1/\mu_s'$ from the light source).^{12–16,18,19} For the study of contaminants in drinking water, we consider samples where light scatters only a few times, known as the single or intermediate scattering regime. The scattering in the system is determined by the concentration of insoluble particles, their size, and the geometry of the system.^{20,21} Higher concentrations of insoluble particles will result in more scattering events.²² To verify our scattering regime, we calculated the optical depth (OD), a parameter that differentiates between different scattering regimes and is described by

$$\text{OD} = l \cdot (\mu_s + \mu_a) \quad (2)$$

where l is the geometric length.²³ In our work, Intralipid and India ink are used as the contaminants, so the OD was calculated according to their optical properties.²⁴ The results confirm that the concentrations of the contaminants used place the samples in the single-intermediate regime as $\text{OD} < 3$, which is in partial agreement with referenced work.²³ Previously, the IPL point was not observed in the single-intermediate scattering regime, so it is necessary to characterize the angle of the IPL point in this regime. In this paper, the optical system used to detect contaminants in water is presented. Intralipid and India ink were used to control optical properties such as scattering and absorption coefficients. This allows for analysis of the IPL point in the single-intermediate scattering regime, eventually establishing a

relationship between the IPL point, sample diameter, and absorption coefficient.

2. MATERIALS AND METHODS

2.1. Optical Setup. The optical setup includes a continuous wave Ne–He laser with a wavelength of 632.8 nm and 0.8 mW power (HNLS008R, Thorlabs). The light source illuminates the cylindrical sample of contaminated water. The FSP is measured using a photodiode (PD) (SM05PD2B, Thorlabs) with an active area of 13 [mm²]. The PD is placed on a rotating stage to allow measurement at all angles. The PD is fixed at a constant distance of 5 mm from the sample surface, and it takes light intensity readings every 5°. The measurement starting point, when $\theta = 0^\circ$, is where the PD and the laser beam are collinear. To achieve reproducibility between measurements, we controlled the photodiode measurement angle (θ) using a stepper motor with a rotational accuracy of $\pm 0.225^\circ$. PD data are collected by an oscilloscope, sent to MATLAB, and analyzed. The described system is shown in Figure 2.

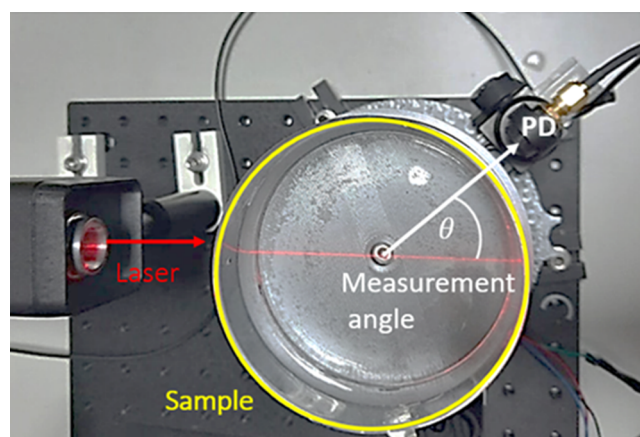


Figure 2. Ne–He laser illuminates the sample and turbid media. The scattered light is collected with a PD at a variety of measurement angles.

2.2. Experimental Description and Sample Preparation. The samples used in this paper were composed of double distilled water (ddw), contaminated with Intralipid, a phospholipid-stabilized soybean oil (Sigma, 68890-65-3). The use of Intralipid allows for the variation of scattering coefficients while holding the absorption coefficient constant.^{24,25} To work within the single and intermediate scattering regime, the scattering coefficient was increased linearly between scans with the incremental addition of Intralipid. The contamination range was from 30 to 46 ppm. Those samples will be referred as the scattering contaminants for the rest of the article. The scattering coefficients of these samples were evaluated using

$$\mu_s = (2.59 \times 10^9) \cdot \lambda^{-2.4} \cdot c \times 10^{-1} \left[\frac{1}{\text{mm}} \right] \quad (3)$$

where c is the concentration of Intralipid in water and λ is the wavelength of the light source in nm.²⁴ To examine the relationship between sample diameter (D) and the IPL point (θ_{IPL}), the scattering contaminants were measured at various D values using the optical setup described in Figure 2. In addition, we examined the relationship between μ_a and the IPL

point properties. The absorption coefficient was varied by linearly adding small concentrations of ink (India ink 1%) to the scattering contaminants, creating mixed samples. The absorption coefficients of each sample were verified using a UV–vis spectrophotometer (Shimadzu, UV-1900, Japan). The optical properties for the different concentrations of Intralipid and ink are presented in Table 1:

Table 1. Optical Properties of the Scattering Contaminants

ink concentration [10^{-6}]	μ_a [mm^{-1}]
0	0
1	0.0196
2	0.0397
3	0.0644
4	0.0836
IL concentration [10^{-6}]	μ_s [mm^{-1}]
30	0.0147
34	0.0166
38	0.0186
42	0.0196
46	0.0225

3. RESULTS

3.1. Self-Calibration Point for Different Sample Diameters. The FSPs of cylindrical scattering contaminants of different diameters and optical properties as presented in Table 1 were measured in the optical system. The results of the measured FSP for each diameter are presented in Figure 3a–f correspond to a sample diameter of $D = 50, 55, 60, 76, 90,$ and 100 mm, respectively.). These results demonstrate the IPL point phenomenon, displayed as a point (circled in red) where position changes but light intensity remains constant. In addition, the results highlight that at angles less than the IPL point, there is an inverse relationship between the scattering coefficient and measured light intensity; that is, before the IPL

point, a sample with a higher μ_s (orange curves) results in a lower intensity reading. However, at angles greater than the IPL point, the trend is flipped, with higher scattering coefficients yielding higher light intensity readings. This characteristic of the IPL point manifests in multiple scattering regimes as well.^{11–13} Furthermore, the back scattering for high angles corresponds to the phase function of Mie scattering that describes these contaminant particles. These findings indicate the presence of the IPL point in the single-intermediate scattering regime. Analysis of the results seen in Figure 3g reveals a linear relationship between the diameter of the samples and the angle at which the IPL point appears. This linear relationship highlights how modifying the diameter can manipulate the IPL angle.

3.2. Impact of Contaminant Concentration on the IPL Point. For this experiment, the FSPs of scattering contaminants with varying concentrations were measured in diameter of 60 mm. Figure 4 presents our results where the IPL point shifts with different concentrations ranges, with higher scattering coefficients leading to a higher IPL point angle closer to the light source. Additionally, the scattering regime changes from single scattering (8–32 ppm, $OD < 3$) to intermediate scattering (64–256 ppm, $OD < 20$) to multiple scattering (384–4000 ppm, $20 < OD$) as the concentration of the contaminant increases. This change can be confirmed by calculating the optical depth using eqs 2 and 3. The IPL point's ability to detect various contamination levels and calibrate each material itself contributes to its versatility in contamination detection.

3.3. Effect of Absorption on the IPL Point. To determine the impact of the absorption coefficient on the IPL point, the FSPs of the 90 mm diameter mixed samples were considered. First, a control sample of scattering contaminants without ink was measured. Next, scattering contaminant samples with incrementally increasing absorption were measured, corresponding to ink concentrations of 1–4 ppm. The measurements of the FSPs are presented in Figure

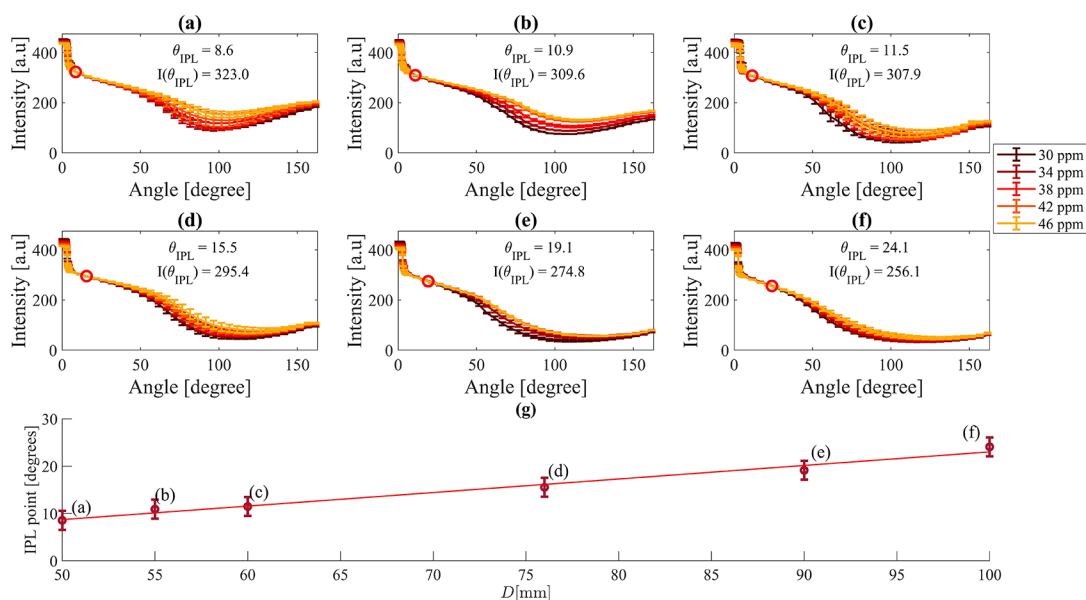


Figure 3. Measurements of the FSP for Intralipid contaminated samples with different diameters while the IPL point is evident within the red mark. (a–f) correspond to a sample diameter of $D = 50, 55, 60, 76, 90,$ and 100 mm, respectively. (g) shows the dependency of sample diameter on the IPL point for the same scattering properties, with each point on the graph corresponding to the respective sample.

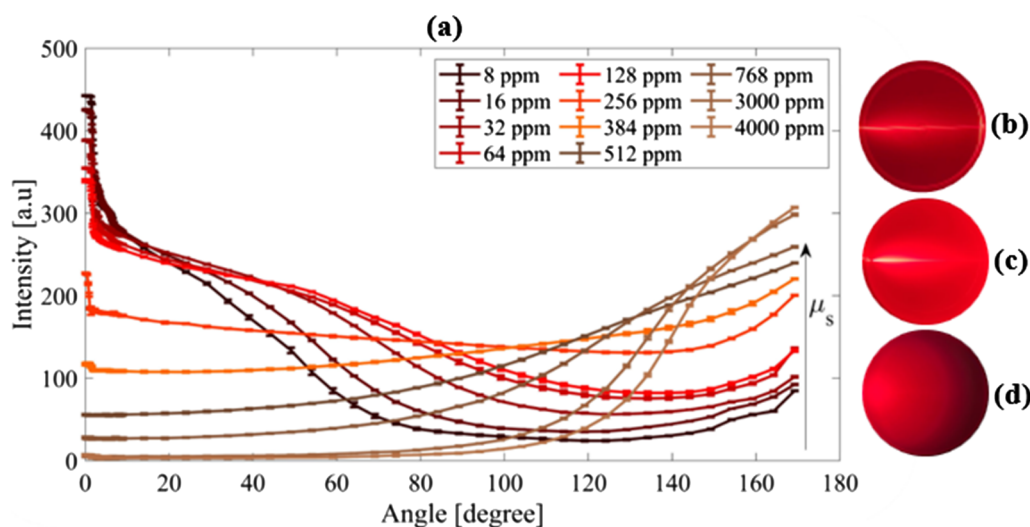


Figure 4. (a) FSP of 60 mm diameters scattering contaminants for a wide range of μ_s . The following photos depict irradiated scattering contaminants at different concentrations: (b) 32 ppm, OD = 0.96 (single scattering), (c) 128 ppm, OD = 3.78 (intermediate scattering), and (d) 3000 ppm, OD = 88.16 (multiple scattering).

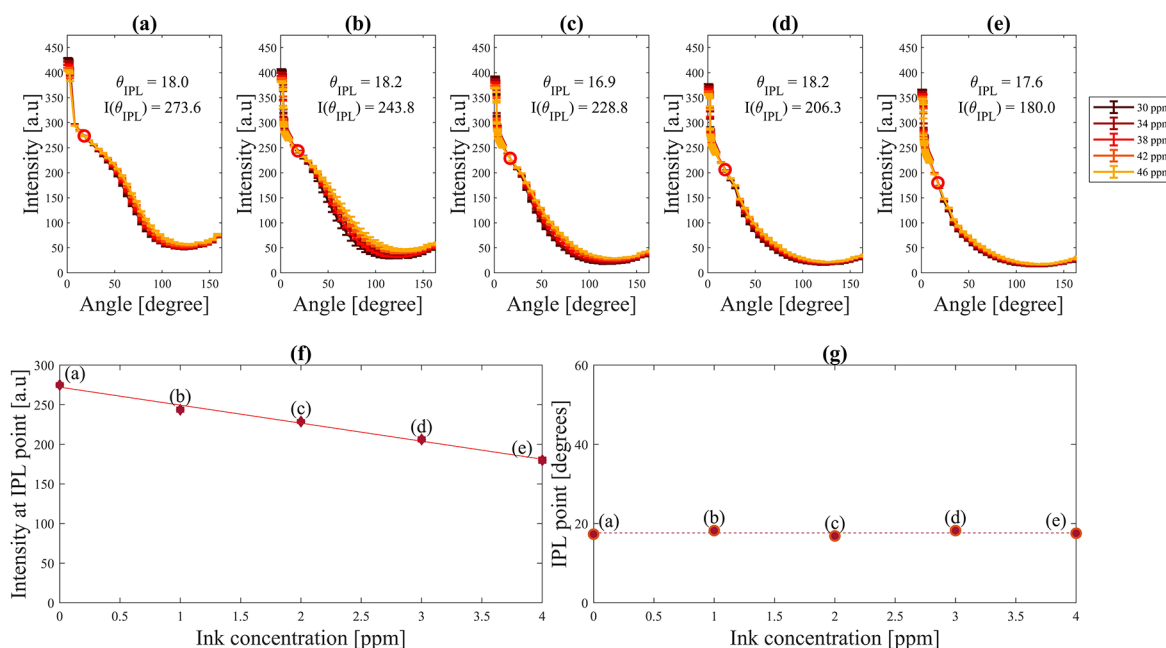


Figure 5. Measurements of the FSPs for mixed samples in $D = 90$ [mm]. The absorption coefficient is increasing linearly from (a–e) according to Table 1. The IPL point is located at the red mark. The influence of the absorption (ink concentration) on the intensity reading at the IPL point (f) and on the IPL angle (g).

5a–e. The IPL point, circled in red, maintains the same angle as the intensity reading decreases with increasing absorption. Analysis of the intensity readings and IPL angles shows that regardless of the absorption coefficient, the IPL angle occurs at an average position of 17.64° with a standard deviation of 0.58° . Additionally, the intensity readings at the IPL point decrease linearly with an increase in ink concentration, indicating that as the μ_a increases, $I(\theta_{\text{IPL}})$ decreases. This phenomenon indicates that the IPL point is the only position where absorption can be extracted without the influence of scattering. This behavior of the IPL point and the linear trend related to its intensity under varying absorption coefficients is consistent with previous work,¹⁵ and this property allows for

the detection of and distinguishing between scattering and absorbing contaminants.

3.4. Detecting Contaminants Using the IPL Point. To differentiate between the two contaminants, Intralipid and India ink, the FSPs of the mixed samples were analyzed (Figure 5), showing impact of both absorption and scattering. Nonetheless, since the IPL point separates the absorption from the scattering, the parameters that described the impact of absorption were isolated. Moreover, studying absorption and scattering separately revealed that scattering affects the shape of the FSP, while absorption affects its attenuation. By incorporating this theory, the analysis indicates that subtracting the minimum intensity reading from the intensity at the IPL point describes the influence of absorption on the FSP. Next,

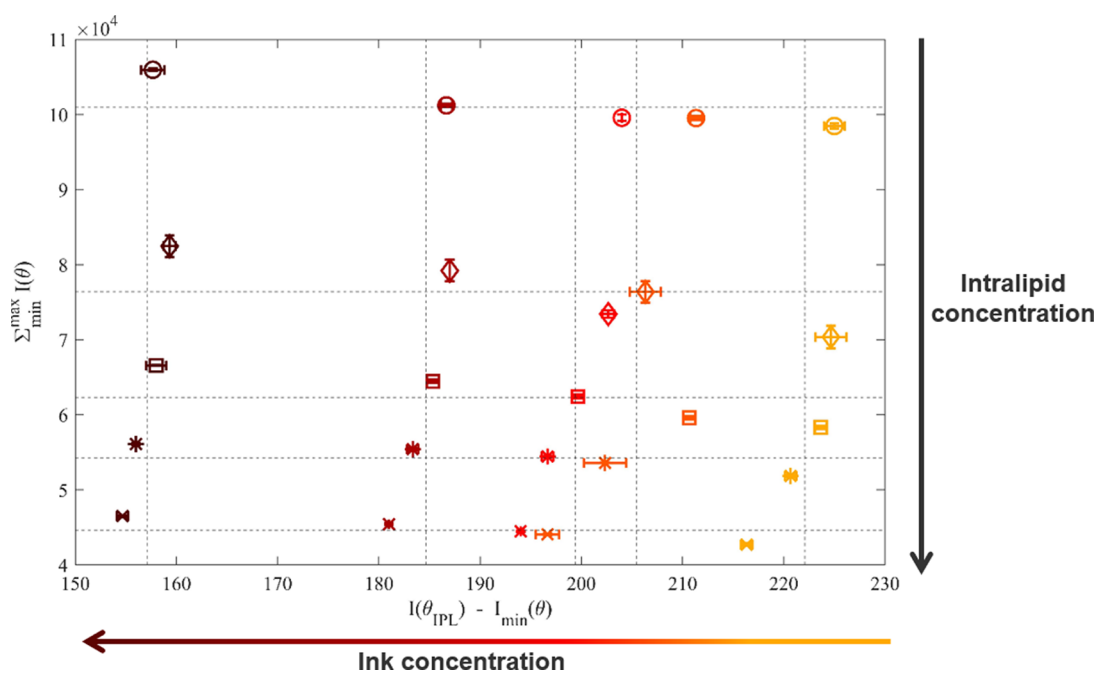


Figure 6. Grid analysis for the detection of two types of contamination. The colors represent different concentrations of ink (0, 1, 2, 3, and 4 ppm), the darker the color, the higher the concentration. The ticks correspond to the Intralipid concentration (“circle,” “diamond,” “square,” “asterisk”, and “cross” corresponding to 30, 34, 38, 42, and 46 ppm, respectively).

to illustrate the influence of the scattering on the intensity, we discovered that the summation of the intensity reading from its maximum value to the minimum conveys the effect of scattering on the FSP. The results of the analysis, shown in Figure 6, classify each sample by the contaminant type and its respective concentration. This results in a grid pattern (dashed lines), where the x and y axes are proportional to the ink and Intralipid concentrations, respectively. This enables the detection of each sample, ink and Intralipid of concentrations between 1–4 and 30–46 ppm, respectively. Error in the analysis where samples are not aligned with extrapolated grid lines can be attributed to errors in sample preparations and differences between individual water samples. Nevertheless, these findings show the successful detection of each sample’s contamination and its concentration in a real time measurement using the IPL phenomenon.

4. DISCUSSION AND CONCLUSIONS

In this study, we demonstrated the existence of the IPL point in the single-intermediate scattering regime using a specific range of Intralipid concentrations (30–46 ppm). Furthermore, we have demonstrated a linear relationship between the IPL point angle and the sample diameter in the single-intermediate scattering regime. To be precise, we found that as the diameter of the scattering contaminants increases, the angle at which the IPL point appears increases. However, since we have only tested the linear ratio for this scattering regime using Intralipid, we cannot assume that it applies to all contaminants. In addition, we have shown that as the absorption coefficient increases, the intensity reading at the IPL point decreases, but the IPL angle remains constant. Finally, we demonstrate how the IPL point can be used to find the absorption coefficient in the single-intermediate scattering regime when the DPF is known. This was achieved by using the ratio between the absorption and control samples while accounting for dark measurement. For this calculation, we employed a numerical

estimate of the DPF. Paired with the assessed DPF, these ratios were used to calculate the absorption coefficient according to eq 1. The resulting values (red diamonds in Figure 7) were

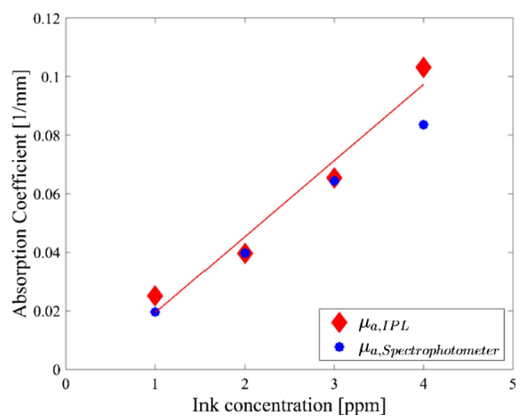


Figure 7. Relationship between the absorption coefficient and the intensity reading in the IPL point divided by the intensity reading in the IPL point without absorbance.

found to be in good agreement with measurements obtained using a UV–vis spectrophotometer (blue circles). This indicates that the IPL point can be used to extract optical properties and become an absolute unit of measurement of the contaminant concentration.

However, these results require further research to verify that the estimated DPF used in this experiment is correct and indeed constant. Additionally, the absorption coefficients in these findings were controlled using India ink, so further research with a different absorber must be conducted to verify the trend. Despite this, our results support the idea that the IPL point can be a valuable tool for determining the optical

properties of materials and for the classification of multiple contaminants in one real-time measurement.

AUTHOR INFORMATION

Corresponding Author

Dror Fixler – The Faculty of Engineering and the Institute of Nanotechnology and Advanced Materials, Bar Ilan University, Ramat Gan 5290000, Israel; orcid.org/0000-0003-0963-7908; Email: Dror.Fixler@biu.ac.il

Authors

Alon Tzroya – The Faculty of Engineering and the Institute of Nanotechnology and Advanced Materials, Bar Ilan University, Ramat Gan 5290000, Israel

Shoshana Erlich – School of Engineering, Rutgers University, New Brunswick, New Jersey 08901-8554, United States

Hamootal Duadi – The Faculty of Engineering and the Institute of Nanotechnology and Advanced Materials, Bar Ilan University, Ramat Gan 5290000, Israel

Complete contact information is available at:

<https://pubs.acs.org/10.1021/acsomega.3c01977>

Author Contributions

The research conceptualization was formed by D.F. In addition, D.F. and H.D. were responsible for the research supervision methodology. The samples preparation (scattering contaminants and mixed samples) as well as the experiments was done by S.E. and A.T. The investigation and optical characterization of the samples and data analysis was done by A.T. The final validation was done by A.T. and H.D. The writing of the first draft was done by A.T. and S.E. while D.F. and H.D. were responsible for the review and editing for improving the paper.

Notes

The authors declare no competing financial interest.

ABBREVIATIONS

FSP, full scattering profile; IPL, iso-pathlength; OD, optical depth; PD, photodiode; ddw, double distilled water; IL, intralipid

REFERENCES

- (1) World Health Organization. *Guidelines for drinking-water quality: second addendum. Vol. 1, Recommendations*; World Health Organization: 2008.
- (2) Borok, A. *Turbidity Technical Review: Summary of Sources, Effects, and Issues Related to Revising the Statewide Water Quality Standard for Turbidity*; Oregon Department of Environmental Quality: 2014.
- (3) Kitchener, B. G.; Wainwright, J.; Parsons, A. J. A review of the principles of turbidity measurement. *Prog. Phys. Geogr.* **2017**, *41*, 620–642.
- (4) Morais, I. P.; Tóth, I. V.; Rangel, A. O. Turbidimetric and nephelometric flow analysis: concepts and applications. *Spectrosc. Lett.* **2006**, *39*, 547–579.
- (5) Wang, P.; Wang, X.; Yu, F.; Gui, H.; Kong, D.; Khan, P.; Wang, H. A Real-Time Water Quality Measurement Instrument for Simultaneously Detecting Turbidity and Particle Size by Using Single-Photon Counting Technique. *IEEE Trans. Instrum. Meas.* **2022**, *77*, 1.
- (6) Tomperi, J.; Isokangas, A.; Tuuttila, T.; Paavola, M. Functionality of turbidity measurement under changing water quality and environmental conditions. *Environ. Technol.* **2022**, *43*, 1093–1101.

(7) Yousif, M.; Burdett, H.; Wellen, C.; Mandal, S.; Arabian, G.; Smith, D.; Sorichetti, R. J. An innovative approach to correct data from in-situ turbidity sensors for surface water monitoring. *Environ. Model. Softw.* **2022**, *155*, No. 105461.

(8) Landers, M. N.; Sturm, T. W. Hysteresis in suspended sediment to turbidity relations due to changing particle size distributions. *Water Resour. Res.* **2013**, *49*, 5487–5500.

(9) Shi, Z.; Chow, C. W. K.; Fabris, R.; Liu, J.; Jin, B. Applications of Online UV-Vis Spectrophotometer for Drinking Water Quality Monitoring and Process Control: A Review. *Sensors* **2022**, *22*, 2987.

(10) World Health Organization. *Water quality and health-review of turbidity: information for regulators and water suppliers*; World Health Organization: 2017.

(11) Duadi, H.; Feder, I.; Fixler, D. Linear dependency of full scattering profile isobaric point on tissue diameter. *J. Biomed. Opt.* **2014**, *19*, No. 026007.

(12) Feder, I.; Wróbel, M.; Duadi, H.; Jędrzejewska-Szczerska, M.; Fixler, D. Experimental results of full scattering profile from finger tissue-like phantom. *Biomed. Opt. Express* **2016**, *7*, 4695–4701.

(13) Feder, I.; Duadi, H.; Fridman, M.; Dreifuss, T.; Fixler, D. Experimentally testing the role of blood vessels in the full scattering profile: solid phantom measurements. *J. Biomed. Photon. Eng.* **2016**, *2*, 40301.

(14) Feder, I.; Duadi, H.; Chakraborty, R.; Fixler, D. Self-calibration phenomenon for near-infrared clinical measurements: theory, simulation, and experiments. *ACS Omega* **2018**, *3*, 2837–2844.

(15) Feder, I.; Duadi, H.; Fixler, D. Single wavelength measurements of absorption coefficients based on iso-pathlength point. *Biomed. Opt. Express* **2020**, *11*, 5760–5771.

(16) Duadi, H.; Feder, I.; Fixler, D. Influence of detector size and positioning on near-infrared measurements and ISO-pathlength point of turbid materials. *Front. Phys.* **2021**, *9*, 43.

(17) Oshina, I.; Spigulis, J. Beer–Lambert law for optical tissue diagnostics: current state of the art and the main limitations. *J. Biomed. Opt.* **2021**, *26*, No. 100901.

(18) Feder, I.; Duadi, H.; Fixler, D. Effect of Spatial Modulated Light on Position of Self-Calibration Point. *IEEE Photon. J.* **2021**, *13*, 1–5.

(19) Duadi, H.; Feder, I.; Fixler, D. Near-infrared human finger measurements based on self-calibration point: Simulation and in vivo experiments. *J. Biophotonics* **2018**, *11*, No. e201700208.

(20) Hulst, H. C.; van de Hulst, H. C. *Light scattering by small particles*; Courier Corporation: 1981.

(21) Bohren, C. F.; Huffman, D. R. *Absorption and scattering of light by small particles*; John Wiley & Sons: 2008.

(22) Hahn, D. W. *Light scattering theory*; Department of Mechanical and Aerospace Engineering, University of Florida: 2009.

(23) Berrocal, E.; Sedarsky, D. L.; Paciaroni, M. E.; Meglinski, I. V.; Linne, M. A. Laser light scattering in turbid media Part I: Experimental and simulated results for the spatial intensity distribution. *Opt. Express* **2007**, *15*, 10649–10665.

(24) Van Staveren, H. J.; Moes, C. J.; van Marie, J.; Prahl, S. A.; Van Gemert, M. J. Light scattering in Intralipid-10% in the wavelength range of 400–1100 nm. *Appl. Opt.* **1991**, *30*, 4507–4514.

(25) Flock, S. T.; Jacques, S. L.; Wilson, B. C.; Star, W. M.; van Gemert, M. J. Optical properties of Intralipid: a phantom medium for light propagation studies. *Lasers Surg. Med.* **1992**, *12*, 510–519.